15B.3 Forecasting and Monitoring Intense Thunderstorms in the Hindu Kush Himalayan Region: Spring 2018 Forecasting Experiment

Jonathan L. Case*[1], Patrick N. Gatlin[2], Jayanthi Srikishen[3], Jeffrey Knockerbocker[4], Jordan R. Bell[5], Roger E. Allen[6], Paul J. Meyer[2], Daniel J. Cecil[2], and Walter A. Petersen[2]

[1]ENSCO, Inc., Huntsville, AL; [2]NASA Marshall Space Flight Center, Huntsville, AL;
[3]Universities Space Research Association, Huntsville, AL; [4]Spatial Informatics Group, Pleasanton, CA;
[5]University of Alabama – Huntsville; Huntsville, AL; [6]Jacobs ESSCA; Huntsville, AL

1. INTRODUCTION

Some of the most intense thunderstorms on the planet occur in the Hindu Kush Himalayan (HKH) region of South Asia (Zipser et al. 2006; Romatschke et al. 2010) — where many organizations lack the capacity needed to predict, observe and/or effectively respond to the threats associated with high-impact convective weather. Among the hazards include tornadoes, damaging straight-line winds (known as Nor'westers in the HKH region), large hail, and flash flooding, which typically peak in the pre-wet-monsoon season (~March through May; Das et al. 2014). Previous studies have documented a disproportionately large number of casualties associated with intense thunderstorms in this region (e.g., Bikos et al. 2016; Bista 1989; Holle 2010); therefore, the goal of this project is to increase situational awareness of these hazards through short-term modeling and satellite assessment tools.

As part of the NASA SERVIR Applied Science Team, this project combines innovative numerical weather prediction (NWP) strategies, satellite-based precipitation products, and land-imagery techniques into a high-impact weather assessment toolkit (HIWAT). The HIWAT is being developed with the goal of transitioning capabilities to weather-sensitive agencies in the HKH region, in order to improve situational awareness and warning decision support. The short-term NWP strategies involve developing real-time regional deterministic and convection-permitting ensemble model guidance, similar to previous Spring Experimental Forecast Program campaigns at the NOAA Hazardous Weather Testbed (e.g., Clark et al. 2012), as well as the now-retired National Center for Atmospheric Research experimental ensemble prediction system (Schwartz et al. 2015).

The strategy of the forecast component of HIWAT is to generate a daily deterministic simulation that produces severe weather composite indices over a targeted area of the HKH region, initially focusing on Nepal, Bangladesh, and northeastern India during Spring 2018. The ensemble system outputs products similar to the Storm-Scale Ensemble of Opportunity at the National Centers for Environmental Prediction (NCEP) Storm Prediction Center (i.e., "paintball" maps, neighborhood probabilities of specific convective hazards, diurnal summary plots, etc.) to depict the most likely areas for severe weather over a 48-hour outlook. Satellite products from the Global Precipitation Mission (GPM) and land-cover processing techniques will then be used to observe convective characteristics and provide datasets to aid in potential damage assessment and recovery activities following an event.

This extended abstract provides an overview of the implementation of a real-time Spring Forecasting Experiment over the HKH region during March to May 2018. The cloud computing hardware and modeling software system are presented in Section 2; details of the ensemble modeling system configuration are described in Section 3; the real-time Numerical Weather Prediction (NWP) experiment design is explained in Section 4, along with preliminary results of severe weather events focusing on northeastern India, Nepal, and Bangladesh in Section 5. The paper concludes with a summary and discussion of future plans for the remainder of the funded project.

2. COMPUTING HARDWARE AND NWP MODEL

2.1 System Hardware

For the Spring 2018 Forecasting Experiment (and for future projects requiring extensive computing resources), NASA SERVIR procured a computational cluster to provide its internationally-focused projects with a "cloud-like" environment. Managed by Spatial Informatics Group, the SERVIR Operational Cluster Resource for Applications - Terabytes for Earth Science (SOCRATES) computational environment provides high-end parallel computing for running intensive, NWP configurations at convection-permitting resolutions (i.e., convection-allowing models [CAM]) for severe thunderstorm forecasting activities over South Asia.

Our computing instance on SOCRATES consists of 13 nodes each with dual 16x2 CPU Intel E5-2683v4 2.1-GHz processors (32 cores per node) for a total of 416 cores. The model runs are launched from one of the nodes acting as the "master node". Each model simulation runs on a separate node with 128 GB of RAM, a virtualized guest Operating System Ubuntu 16.04 LTS with Hyper-Threading disabled, on top of the VMware vSphere Hypervisor (ESXi 6.5). Each node has a shared 1.2 TB of solid-state drive (SSD) for fast I/O throughput and 96 TB of hard drive for long term storage via Network File System (NFS). A 10 Gbps local area network serves as communication between the compute nodes. No high-speed interface for message passing exists in the initial configuration of SOCRATES.

**Corresponding author address:* Jonathan Case, ENSCO, Inc., 320 Sparkman Dr., Room 3000B, Huntsville, AL, 35805. Email: Jonathan.Case-1@nasa.gov

Figure 1. SOCRATES cloud-emulating computing hardware rack consisting of [currently] 16 computational nodes with 32 cores per node, used for the Spring 2018 Hindu Kush Himalayan Forecasting Experiment.

2.2 NWP Modeling Software

Version 15 of the Unified Environmental Modeling System (UEMS; available online at http://strc.comet.ucar.edu/ software/uems/) was used as the NWP software of choice for the Spring 2018 Forecasting Experiment. The UEMS version 15 is based on version 3.7.1 of the community Weather Research and Forecasting (WRF) NWP modeling system (Skamarock et al. 2008), and features a streamlined process for quickly and easily installing, configuring, and executing the WRF model on a Linux-based operating environment without requiring of purchasing licensed compilers and installing complicated supporting library packages. The UEMS also includes post-processing utilities for generating numerous derived fields and graphical products. This combination of features in the UEMS made it the optimal choice for setting up and running the ensemble modeling system on SOCRATES in an expeditious manner. In fact, the SOCRATES operating system and supporting software only became available in late January 2018, and by late February, the ensemble modeling components were up and running in real-time, ready for the March–May campaign.

3. ENSEMBLE MODEL CONFIGURATION

The Spring 2018 Forecasting Experiment ensemble model configuration had an objective to provide day-1 and day-2 real-time forecast guidance of pre-monsoon intense thunderstorm hazards via a CAM nested grid configuration. The ensemble system must have adequate variability or spread in the simulations to capture errors and uncertainty in the solution. The system must also support a sufficiently fast run-time performance to minimize latency and thereby provide products with potential utility to experimental operations in the HKH region. Given the computational constraints and scientific/real-time [operational] objectives of the project, we chose a 12-member ensemble system as a viable experimental solution. Because of the lack of hardware for inter-node high-speed network (e.g., InfiniBand or Myrinet) for the Spring 2018 Experiment, the model grid was designed to run an ensemble member on a single SOCRATES compute node with a run-time performance of approximately 10% of real time. Therefore, 12 compute nodes were dedicated to run each of the 12 members comprising the ensemble forecasting system, for optimal performance on SOCRATES in a real-time mode.

The model grid domain was subsequently designed to provide CAM guidance in a nested grid over a focus region covering all of Nepal, Bangladesh, and much of northeastern India, while still running an individual ensemble member sufficiently fast in real time on a single compute node. The resulting 12-km/4-km mesh grid configuration is shown in Figure 2, with applicable details common to each ensemble member summarized in Table 1.

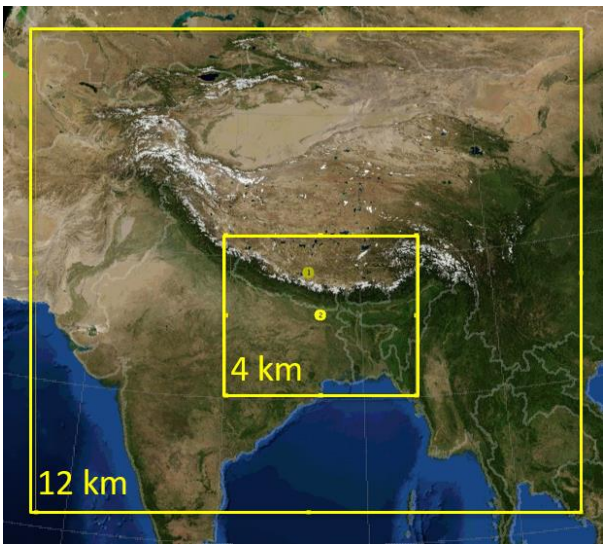

Figure 2. Nested grid configuration of the UEMS/WRF ensemble for the Spring 2018 Forecasting Experiment. Configuration details are summarized in Table 1.

Table 1. Select details of the nested grid configuration common to each ensemble member.

Feature	12-km outer grid	4-km nested grid
W-E points	351	367
S-N points	321	322
Vertical levels	42	
Domain top	20 hPa	
Initialization	1800 UTC daily	
Integration	48 hours daily	
Dynamic timestep	60 s	20 s
Cumulus Parm	Kain-Fritsch	None
Shortwave radiation	RRTM-G	
Longwave radiation	RRTM-G	

To achieve a reasonable amount of spread in the ensemble system, a combination approach of initial condition and physical parameterization variability is applied. Each individual member has a different set of initial and boundary conditions from the NCEP/Environmental Modeling Center (EMC) Global Forecast System (GFS; Han and Pan 2011) for member HKH1, and from the 21-member NCEP/EMC Global Ensemble Forecast System (GEFS; Guan et al. 2015; Zhou et al. 2017) for members HKH2-12. The GEFS members for initializing HKH2-12 were arbitrarily chosen by taking every other member sequentially beginning with GEFS03, as summarized in Table 2. The physical parameterization variations were chosen based on the type of schemes that affect the development of, or are impacted by model moist convective processes. Thus, we chose to vary the planetary boundary layer (PBL) and microphysical (MP) parameterization schemes that represent turbulent kinetic energy and mixed-phase cloud and precipitation processes, respectively. The resulting matrix of initial/boundary condition and physical parameterization variations among the ensemble members (Table 2) was thus applied on a daily basis, from which specific ensemble system products and probabilities were derived, as described in the next section.

A daily initialization at 1800 UTC with 48-hour integration length were chosen in order to (1) provide ~6 hours of model "spin-up" prior to local sunrise (~0000 UTC) leading into the first diurnal heating cycle, and (2) capture two full diurnal heating cycles for day-1 and day-2 intense thunderstorm guidance. The few hours of spin-up is necessary since no data assimilation or diabatic initialization techniques were implemented for the model simulations, thus no microphysical properties are available in the initial conditions. Each ensemble member outputs the model results at hourly intervals.

The 1200 UTC cycle of the GFS/GEFS provided initial and boundary conditions for the 1800 UTC initialization of the UEMS/WRF runs. Initial conditions came from the 6-hour GFS/GEFS forecasts, with 3- [6-]hourly boundary conditions provided by 0.25-deg resolution GFS [0.5-deg resolution GEFS] model output. The previous cycle of the GFS/GEFS was chosen in order to expedite the ensemble system and maximize the time-relevant model output results. The 12 ensemble members began running between 1715-1800 UTC each day, staggered every few minutes to avoid pre-processing jobs interfering with one another on the master node. To further expedite ensemble output availability in real time, concurrent post-processing was performed on the master node for all 12 ensemble members, while each member ran on its own dedicated compute node. That way, most of the post-processing was ready as the model simulations were completed.

Table 2. Matrix of initial/boundary conditions, and planetary boundary layer (PBL) and microphysical (MP) parameterization variations comprising the 12-member ensemble system. PBL schemes: YSU (Yonsei University; Hong et al. 2004), MYJ (Mellor-Yamada-Janjic; Janjic 1994), and MYNN2 (Mellor-Yamada Nakanishi and Niino Level 2.5 closure; Nakanishi and Niino 2006). MP schemes: Godd (Goddard 6-class with graupel; Lang et al. 2007, 2011), Lin 6-class (Lin et al. 1983) [Thompson et al. 2008 from 1-28 March 2018], WSM6 (WRF Single-Moment 6-class; Hong and Lim 2006), and Morr (Morrison double-moment; Morrison et al. 2009).

MP → / PBL ↓	Godd	Lin	WSM6	Morr
YSU	HKH1: GFS	HKH2: GEFS 03	HKH3: GEFS 05	HKH4: GEFS 07
MYJ	HKH5: GEFS 09	HKH6: GEFS 11	HKH7: GEFS 13	HKH8: GEFS 15
MYNN2	HKH9: GEFS 17	HKH10: GEFS 19	HKH11: GEFS 02	HKH12: GEFS 04

4. SPRING 2018 ENSEMBLE PRODUCT SUITE

4.1 Thunderstorm Hazard Proxy Fields

Following Kain et al. (2010), we developed a series of ensemble products based on proxy simulated fields representing specific convective hazards:

- ***Composite reflectivity*** to represent overall convective intensity,
- ***Lightning Forecast Algorithm*** (LFA; McCaul et al. 2009) to represent lightning threat,
- ***Maximum output interval 10-m wind speed*** to represent damaging straight-line wind threat,
- ***Maximum output interval total column graupel*** to represent hail threat,
- ***Maximum output interval 2-5 km and 1-6 km updraft helicity*** (Kain et al. 2008) to represent the mesocyclone/tornado threat, and
- ***Accumulated precipitation*** focusing on 1-h and 3-h intervals (as well as longer accumulation intervals) to represent [flash] flooding threat.

These convective hazard proxy fields form the basis for all subsequent ensemble products described in the next sub-section.

4.2 Ensemble Product Descriptions

The ensemble product suite for the Spring 2018 intense thunderstorm Forecasting Experiment followed similar CAM product suites in the Continental U.S. (Clark

et al. 2012; Schwartz et al. 2015). Besides "standard" ensemble fields such as postage stamp displays, ensemble mean, minimum, maximum, and spread (most applicable to continuous fields such as 2-m temperature, 2-m dew point temperature, and Convective Available Potential Energy [CAPE]), our product suite featured 2D "paintball" and probability fields that help to capture areas most likely to experience intense thunderstorm hazards. The paintball products apply a priori thresholds to the proxy convective fields listed above, and plot each ensemble member's threshold objects with a different color and level of transparency. Paintball plots showing "clustered" objects indicate a higher likelihood of hazards occurring in that region, according to the ensemble solution. Fewer objects and/or less over-lapping suggests lower confidence in the hazard.

The paintball concept for intense thunderstorm hazards can then be extended to probability products, of which our product suite generated three types:

- Grid point probability: Simple probability of a threshold being exceeded at each grid point, most appropriate for continuous variables such as temperature or CAPE.
- Neighborhood probability: Search for threshold hits within a neighborhood window box centered on grid point, then re-compute probability.
- Probability Matched Mean (PMM; Ebert 2001; Clark 2017): Re-assignment of ensemble mean field by replacing ranked ensemble mean values with every *nth* value from the ranked histogram of all ensemble members combined.

For the Spring 2018 experiment, we used a +/- 20-km neighborhood box, but multiple neighborhoods can be applied. Neighborhood probability is most suitable for evaluating thunderstorms hazards with a small geographical footprint, since these features often do not overlap between individual ensemble members. The PMM is commonly applied to fields such as accumulated precipitation and composite reflectivity. While the ensemble mean tends to verify best spatially compared to individual ensemble members (Ebert 2001), averaging the individual ensemble members tends to "wash out" the amplitude, thereby over-[under-] representing light [heavy] intensities in the ensemble mean field. The PMM essentially builds back the high-amplitude features found in the individual members while trimming back the over-production of lighter intensities. All of the products described above were generated at hourly intervals from 1-48 hours.

4.3 Day-1 and Day-2 Daily Summaries

In addition to the hourly products, day-1 and day-2 summary fields were generated to provide a "quick look" into the character of intense thunderstorm activity during the first and second 24-hour periods of the ensemble forecast system, respectively. To create the daily summary plots, the maximum quantities of any thunderstorm hazard were stored into a 2D array over the first and second 24-hour period. Thresholds were then applied to create day-1 and day-2 probability fields that depict where thunderstorm hazards will exceed the thresholds at any time during the 24-hour period. These daily summary probabilities can be helpful to focus on regions most likely to experience intense thunderstorm hazards any time during the first and second 24-hour periods (similar to an SPC day-1 or day-2 convective outlook). After a quick examination of the day-1/day-2 hazards, forecasters could then examine the hourly ensemble products to gain an understanding of the most likely timing of the intense thunderstorm hazards.

4.4 Visualization

Graphical fields were hosted on an internal (but publically facing) project web page that was facilitated by the NASA Short-term Prediction Research and Transition (SPoRT) Center, for displaying select deterministic output from ensemble member 1, and for numerous ensemble fields, paintball maps, and probabilities (Figure 3), in both real-time and archive mode. Graphics were populated in real-time as the ensemble forecasts were generated and post-processed. Also, all daily archived simulations for the Spring Forecasting Experiment can be accessed from the web interface.

Additionally, a web mapping service called "Tethys" has been developed, in which ensemble products can be visualized as a layer on top of other geo-navigated datasets. An important strength of Tethys when displaying the hourly [deterministic or ensemble] products is that the user can interactively query the output over defined polygons or selected points, and the Tethys application will quickly provide time-series graphs of the output field or thunderstorm hazard probabilities. An example of the Tethys capabilities for the 29 March 2018 ensemble simulation is shown in Figure 4. This example highlights the user-interactive nature of Tethys, showing a time-series of supercell / mesocyclone probabilities as averaged over the user-defined polygon region, as well as time series at select user-defined points within the interactive interface (upper-left of Figure 4). Select ensemble probabilities, precipitation products, and deterministic fields from HKH1 will be transitioned into the Tethys interface in real time for future increased efficiency in using the ensemble output products by operational weather forecasters in Nepal and Bangladesh.

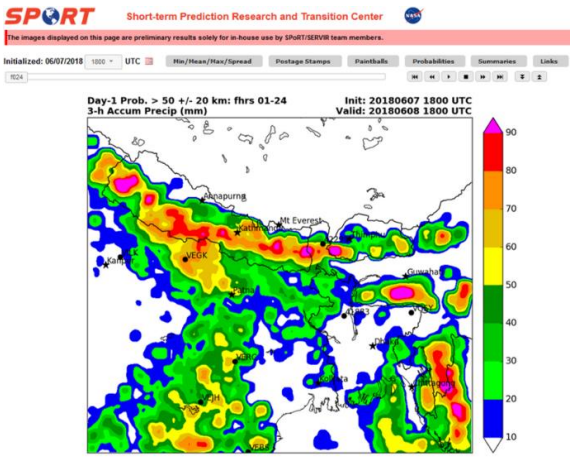

Figure 3. Screen capture of the real-time web page hosting ensemble output products for the collection of daily forecasts during the Spring 2018 experiment.

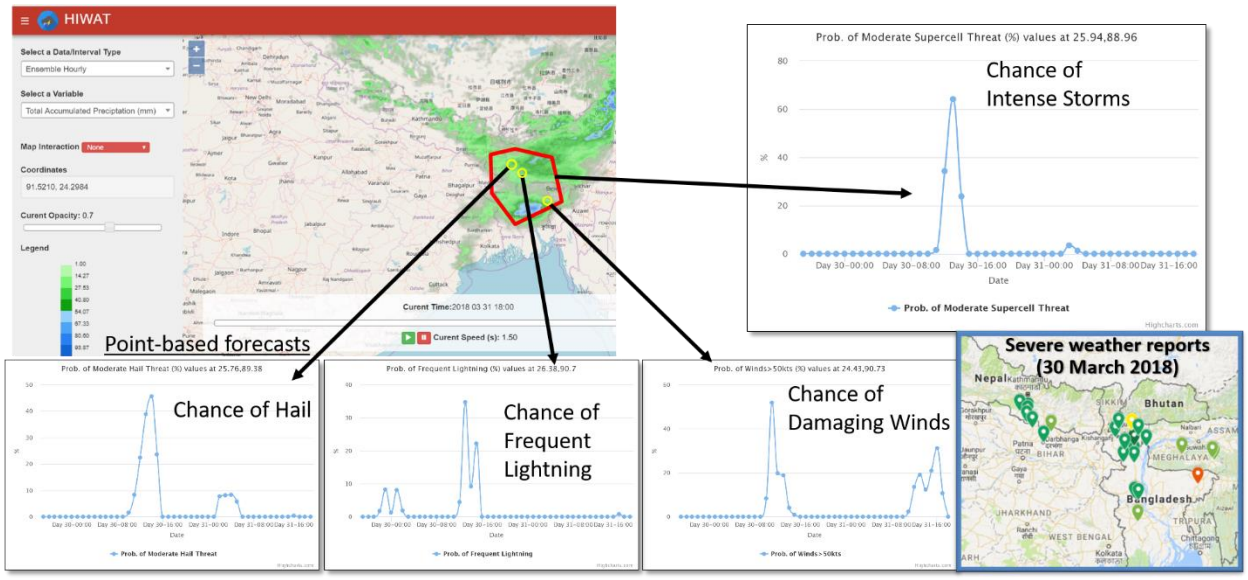

Figure 4. NASA SERVIR "Tethys" application for overlaying HIWAT ensemble model output with other geo-navigated datasets. This example from the 29 March 2018 ensemble simulation shows a time-series of supercell probabilities (based on 2-5 km updraft helicity threshold of 100 m^2 s^{-2}) within a user-defined polygon (red outline in upper-left Tethys interface), as well as hail, lightning, and damaging wind time series probabilities at sampled points (yellow circles in upper-left). Preliminary severe weather reports compiled for 30 March is shown in the lower-right inset.

Table 3. Preliminary list of intense thunderstorm events during the Spring 2018 Forecasting Experiment over the 4-km nested grid HKH region. Days were considered events if one or more human casualities occurred and/or damage was documented by regional media sources.

Event	Location	Lightning	Wind	Hail
29-Mar-18	Bhutan			X
	NE India	X	X	
30-Mar-18	Bangladesh	X	X	X
	Nepal			X
	N India			X
	NE India	X	X	
11-Apr-18	NW India	X	X	
17-Apr-18	N. India	X	X	
21-Apr-18	NE India		X	
22-Apr-18	Bangladesh	X	X	
29-Apr-18	Bangladesh	X		
	N. India	X		
30-Apr-18	Bangladesh	X	X	
2-May-18	N. India	X	X	
6-May-18	Bangladesh	X		
	NE India	X	X	
7-May-18	NE India		X	
9-May-18	Bangladesh	X		
	NE India	X	X	
10-May-18	Bangladesh		X	X
	NE India		X	
11-May-18	Bangladesh	X	X	X
	NE India		X	X
13-May-18	N. India	X	X	
15-May-18	Bangladesh	X		

5. PRELIMINARY RESULTS OF SEVERE WEATHER EVENTS DURING SPRING 2018

The Spring Forecasting Experiment campaign began rather slowly, with very few intense convective events occurring in March. However, a substantial hail, wind and lightning event occurred on 29-30 March in eastern Nepal, northern Bangladesh and northeastern India, followed by numerous severe convective wind events and lightning casualties, especially between mid-April and mid-May. A deadly high wind event occurred in the Kolkata/West Bengal region of southeastern India on 18 April. A particularly intense Nor'wester that created a substantial duststorm affected northwestern and north-central India on 2 May, killing over 100 people with numerous collapsed buildings. [This event occurred primarily west of the nested 4-km grid during the overnight hours of 2-3 May.] Overall, as many as 300 or more people perished as a result of pre-monsoon intense thunderstorm hazards in India, Bangladesh, and Nepal during the Experiment, primarily due to straight-line convective winds and lightning strikes. Table 3 provides a summary of the intense thunderstorm events documented during the Spring 2018 Experiment.

The ensemble forecast initialized on 1800 UTC 29 March captured fairly well the areas of large hail (some nearly 7 cm in diameter—baseball size), damaging convective winds, and lightning observed for the 30 March event. Two regions of substantial graupel [hail proxy] and straight-line wind threats were indicated by the ensemble probability summaries across central / eastern Bangladesh, and eastern Nepal / northern Bangladesh / northeastern India (Figure 5). The regions of high graupel probability exceeding 30 kg m^{-2} spatially correspond well with the large hail reports, given by the green makers in the lower-right inset of Figure 4. Similar analysis and validation will be conducted for as many of the events as possible, through examination of satellite imagery and compilation of storm reports and locations.

Of course, validation of forecast hail and convective wind events is highly dependent on an accurate compilation of damage reports from the field, which is a work in progress for the HKH region. For the events listed in Table 3, the project team members are working with collaborators from Nepal, India, and Bangladesh to document observed casualties and damage reports for these and other potential events not listed. The remote-sensing component of the HIWAT tool will help to document areas of damage and particularly inundation signals associated with flooding events during the upcoming wet monsoon season, through the use of land cover differencing techniques using traditional Low Earth Orbiting satellites and Synthetic Aperture Radar datasets.

6. SUMMARY AND FUTURE PLANS

Our team will continue working with forecasters and collaborators in the HKH region to accurately compile storm reports for the 2018 pre-monsoon intense thunderstorm season. In addition, we will conduct quantitative validation of events [to the degree possible] using Earth Networks Total Lightning Network (ENTLN) data for validating the LFA output. We will also invoke the final product version of the Integrated Multi-satellitE Retrievals for GPM (IMERG) half-hourly rain rates for verifying model accumulated precipitation from individual ensemble members, as well as the ensemble mean and PMM fields.

Future work will also involve transitioning the ensemble product suite in real time into the NASA/SERVIR Tethys application to offer a more interactive tool for querying and sampling the model guidance. The HIWAT ensemble system will continue running through the 2018 summer wet monsoon season to provide experimental quantitative precipitation forecast (QPF) guidance to both forecasters and hydrological modeling applications. The ensemble QPF from the 12 individual members and PMM accumulated precipitation will provide a foundation for generating probabilistic-based streamflow forecasts in the HKH region during the wet monsoon season.

ACKNOWLEDGEMENTS/DISCLAIMERS

This research is funded by NASA's Applied Sciences Capacity Building Program Manager, Dr. Nancy Searby. We would like to thank Dr. Bhupesh Adhikary and the International Centre for Integrated Mountain Development (in Kathmandu, Nepal) for their assistance during this project. Mention of a copyrighted, trademarked or proprietary product, service, or document does not constitute endorsement thereof by the authors, ENSCO Inc., the SERVIR program, the International Centre for Integrated Mountain Development, the National Aeronautics and Space Administration, or the United States Government. Any such mention is solely for the purpose of fully informing the reader of the resources used to conduct the work reported herein.

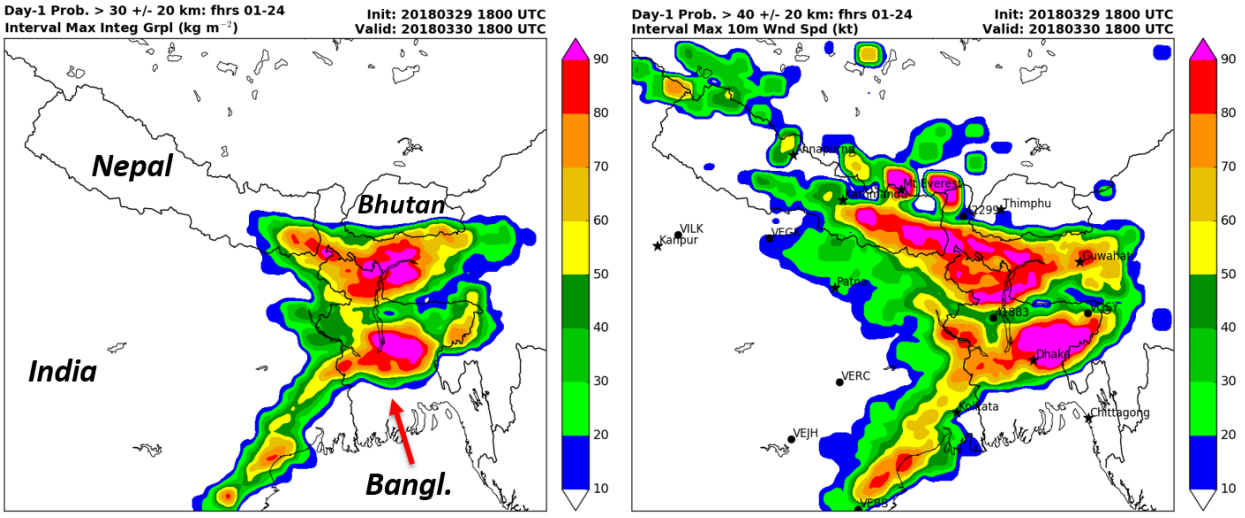

Figure 5. Day-1 neighborhood probability summaries for column-integrated graupel exceeding 30 kg m^{-2} (left), and 10-m wind speed exceeding 20.6 m s^{-1} (40 kt; right), valid for the 24-hour period spanning 1800 UTC 29 March to 1800 UTC 30 March 2018.

REFERENCES

Bikos, D., J. Finch, and J. L. Case, 2016: The environment associated with significant tornadoes in Bangladesh. *Atmos. Res.,* **167,** 183–195, doi:10.1016/j.atmosres.2015.08.002.

Bista, D. B., 1989: Nepal in 1988: Many Losses, Some Gains. *Asian Surv.,* **29,** 223–228, doi:10.2307/2644583.

Clark, A. J., 2017: Generation of ensemble mean precipitation forecasts from convection-allowing ensembles. *Wea. Forecasting,* **32,** 1569-1583, doi: 10.1175/WAF-D-16-0199.1.

Clark, A. J., and Coauthors, 2012: An Overview of the 2010 Hazardous Weather Testbed Experimental Forecast Program Spring Experiment. *Bull. Amer. Meteor. Soc.,* **93,** 55–74, doi:10.1175/BAMS-D-11-00040.1.

Das, S., and Coauthors, 2014: The SAARC STORM: A coordinated field experiment on severe thunderstorm observations and regional modeling over the South Asian region. *Bull. Amer. Meteor. Soc.,* **95,** 603-617, doi:10.1175/BAMS-D-12-00237.1.

Ebert, E. E., 2001: Ability of a poor man's ensemble to predict the probability and distribution of precipitation. *Mon. Wea. Rev.,* **129,** 2461-2480, doi:10.1175/1520-0493(2001)129<2461:AOAPMS>2.0.CO;2.

Guan, H., B. Cui and Y. Zhu, 2015: Improvement of statistical postprocessing using GEFS reforecast information. *Wea. Forecasting,* **30,** 841–854, doi: http://dx.doi.org/10.1175/WAF-D-14-00126.1.

Han, J., and H.-L. Pan, 2011: Revision of convection and vertical diffusion schemes in the NCEP Global Forecast System. *Wea. Forecasting,* **26,** 520–533, doi:10.1175/WAF-D-10-05038.1.

Holle, R. L., 2010: Lightning-caused casualties in and near dwelling and other buildings. *21st International Lightning Detection Conference,* Orlando, Florida, Vaisala, 19 [Available online at "http://www.vaisala.com/Vaisala Documents/Scientific papers/9.Holle-Lightning-Caused.pdf"].

Hong, S.-Y., and J.-O. J. Lim, 2006: The WRF single-moment 6-class microphysics scheme (WSM6). *J. Korean Meteor. Soc.,* **42,** 129-151.

——, S.-Y., Y. Noh, and J. Dudhia, 2006: A new vertical diffusion package with an explicit treatment of entrainment processes. *Mon. Wea. Rev.,* **134,** 2318-2341, doi:10.1175/MWR3199.1.

Janjic, Z. I., 1994: The step-mountain Eta coordinate model: Further developments of the convection, viscous sublayer, and turbulence closure schemes. *Mon. Wea. Rev.,* **122,** 927-945, doi: 10.1175/1520-0493(1994)122<0927:TSMECM>2.0.CO;2.

Kain, J. S., and Coauthors, 2008: Some practical considerations regarding horizontal resolution in the first generation of operational convection-allowing NWP. *Wea. Forecasting,* **23,** 931–952, doi:10.1175/WAF2007106.1.

——, S. R. Dembek, S. J. Weiss, J. L. Case, J. J. Levit, and R. A. Sobash, 2010: Extracting unique information from high-resolution forecast models: Monitoring selected fields and phenomena every time step. *Wea. Forecasting,* **25,** 1536–1542, doi:10.1175/2010WAF2222430.1.

Lang, S., Tao, W.-K., Cifelli, R., Olson, W., Halverson, J., Rutledge, S., Simpson, J., 2007. Improving simulations of convective system from TRMM LBA: easterly and Westerly regimes. *J. Atmos. Sci.,* **64,** 1141-1164.

——, ——, Zeng, X., Li, Y., 2011. Reducing the biases in simulated radar reflectivities from a bulk microphysics scheme: tropical convective systems. *J. Atmos. Sci.,* **68,** 2306-2320.

Lin, Y.-L., R. D. Farley, and H. D. Orville, 1983: Bulk parameterization of the snow field in a cloud model. *J.*

Climate Appl. Meteor., **22,** 1065-1092, doi: 10.1175/1520-0450(1983)022<1065:BPOTSF>2.0.CO;2.

McCaul, E. W., S. J. Goodman, K. M. LaCasse, and D. J. Cecil, 2009: Forecasting lightning threat using cloud-resolving model simulations. *Wea. Forecasting*, **24**, 709–729, doi:10.1175/2008WAF2222152.1.

Morrison, H., G. Thompson, and V. Tatarskii, 2009: Impact of cloud microphysics on the development of trailing stratiform precipitation in a simulated squall line: Comparison of one- and two-moment schemes. *Mon. Wea. Rev.,* **137,** 991-1007, doi:10.1175/2008 MWR2556.1.

Nakanishi, M., and H. Niino, 2006: An improved Mellor–Yamada level-3 model: Its numerical stability and application to a regional prediction of advection fog. *Bound. Layer Meteor.,* **119,** 397-407.

Romatschke, U., S. Medina, and R. A. Houze, 2010: Regional, seasonal, and diurnal variations of extreme convection in the South Asian region. *J. Climate,* **23,** 419–439, doi:10.1175/2009JCLI3140.1.

Schwartz, C. S., G. S. Romine, R. A. Sobash, K. R. Fossell, and M. L. Weisman, 2015: NCAR's experimental real-time convection-allowing ensemble prediction system. *Wea. Forecasting,* **30,** 1645–1654, doi:10.1175/WAF-D-15-0103.1.

Skamarock, W. C., and Coauthors, 2008: : A Description of the Advanced Research WRF Version 3. 123 pp. [Available online at "http://www.mmm.ucar.edu/wrf/ users/docs/arw_v3.pdf"].

Thompson, G., P. R. Field, R. M. Rasmussen, and W. D. Hall, 2008: Explicit forecasts of winter precipitation using an improved bulk microphysics scheme. Part II: Implementation of a new snow parameterization. *Mon. Wea. Rev.,* **136,** 5095-5115, doi:10.1175/2008 MWR2387.1.

Zhou, X., Y. Zhu, D. Hou, Y. Luo, J. Peng, and R. Wobus, 2017: Performance of the new NCEP Global Ensemble Forecast System in a parallel experiment. *Wea. Forecasting,* **32,** 1989-2004, doi:10.1175/WAF-D-17-0023.1.

Zipser, E. J., C. Liu, D. J. Cecil, S. W. Nesbitt, and D. P. Yorty, 2006: Where are the most intense thunderstorms on Earth? *Bull. Amer. Meteor. Soc.,* **87,** 1057–1071, doi:10.1175/BAMS-87-8-1057.